*Vietnam Journal of Science and Technology* ***63*** *(4) (2025) 806-819*

doi:10.15625/2525-2518/17640

# Free vibration of agglomerated carbon nanotube reinforced composite sandwich beam using an enriched finite beam element

**Thi Thom Tran[1, *], Thi Thu Hoai Bui[1], Dinh Kien Nguyen[1, 2]**

[1]*Institute of Mechanics, Vietnam Academy of Science and Technology, 18 Hoang Quoc Viet, Cau Giay, Ha Noi, Viet Nam*

[2]*Graduate University of Science and Technology, Vietnam Academy of Science and Technology, 18 Hoang Quoc Viet, Cau Giay, Ha Noi, Viet Nam*

[*]Email: *ttthom@imech.vast.vn*

Received: 8 November 2022; Accepted for publication: 22 June 2025

**Abstract.** Free vibration of carbon nanotube reinforced composite (CNTRC) sandwich beams, taking into account the effect of CNT agglomeration, is studied using an efficient beam element. The sandwich beams consist of three layers, a homogeneous core and two agglomerated CNTRC face sheets with material properties being estimated by the Eshelby-Mori-Tanaka approach. Based on the trigonometric shear deformation theory, a finite beam element is formulated and used to construct the discretized equation of motion for the beams. To improve the efficiency of the element, hierarchical functions are employed to enrich the conventional Lagrange and Hermite interpolation functions. The numerical investigation shows that the formulated beam element is efficient, and it is capable to give accurate natural frequencies by using a small number of elements. It is also foundation the frequencies of the beams are significantly influenced by the CNT agglomeration, and the increase of CNT reinforcement may not be useful for the beam with severe CNT agglomeration. A parametric study is carried out to investigate the effects of the agglomeration, the volume fraction of CNTs as well as the layer thickness ratio on the vibration of the sandwich beams.

*Keywords:* CNTRC sandwich beam, CNT agglomeration, free vibration, enriched interpolation, finite element method.

*Classification numbers*: 5.4.2, 5.4.5.

## 1. INTRODUCTION

Carbon nanotubes with high aspect ratio, large surface area as well as outstanding mechanical, thermal, and physical properties make them an idea material for reinforcing polymer matrices. Many studies have pointed out that adding small amounts of CNTs to the matrix of a polymer composite can considerably enhance its mechanical properties. However, in most studies the CNTs are considered as aligned single-walled carbon nanotubes (SWCNTs) and estimated through rule of mixture model (ROM) [1 - 5].

CNTs have high aspect ratios and low bending stiffness, making them susceptible to agglomeration within the polymer matrix. To predict the effective properties of composites reinforced by agglomerated CNTs, Shi *et al.* [6] developed a micromechanics model that considers CNTs agglomeration. Free vibration analysis of functionally graded CNT-reinforced composite (FG-CNTRC) beam using Eshelby-Mori-Tanaka (E-M-T) approach are analyzed numerically by Heshmati and Yas [7]. In there, a two parameter micromechanics model [6] is employed to determine the effect of CNTs agglomeration on the elastic properties of randomly oriented CNTRC, and then the effective moduli of the composite are derived from the Mori-Tanaka (M-T) method. Different SWCNTs distributions in the thickness are introduced to determine fundamental frequency of composite beam in [7]. Nejati and Eslampanah [8] studied natural frequency of a thick cantilever beam reinforced by CNTs functionally distributed along the thickness. The generalized differential quadrature method (GDQM) is used to discretize the equations of motion and to implement the boundary conditions. Kamarian *et al.* [9] predicted the free vibration characteristics of FG nanocomposite sandwich beams on Pasternak foundation, considering the agglomeration effect of SWCNTs. The natural frequency analysis of non-uniform CNTRC beams with piezoelectric layers considering CNT agglomeration effect was presented by Kamarian *et al.* [10], using the GDQ technique and Eshelby-Mori-Tanaka approach. Recently, Kiani *et al.* [11] studied the thermo-mechanical buckling of CNTRC beams under a non-uniform thermal loading. The CNTs are orientated randomly and distributed along thickness direction by various symmetric and non-symmetric patterns, and agglomeration of CNTs is incorporated.

This paper is motivated by the lack of studies on the influence of CNT agglomeration on vibration of CNTRC sandwich beams. The core of the sandwich beam is homogeneous, while the two face sheets are made from CNT reinforced composite material. The E-M-T approach is used to estimate the mechanical properties of the beam. Based on the trigonometric shear deformation theory, a two-node beam element is formulated and employed to construct the discretized equation of motion for the beams. The effects of various parameters, including the CNTs agglomeration, volume fraction of CNTs and layer thickness ratio on the vibrational behavior of the sandwich beams are examined in detail and highlighted.

## 2. BEAM REINFORCED WITH AGGLOMERATED CNTS

Figure 1 shows a simply supported sandwich beam with length *L*, rectangular cross section $(b \times h)$. The core of the sandwich beam is made of homogeneous material while the face sheets are material reinforced by CNTs. The Cartesian coordinate system in Figure 1 is chosen such that the *x*-axis is on the beam's mid-plane, and the *z*-axis is perpendicular to the mid-plane and it directs upward.

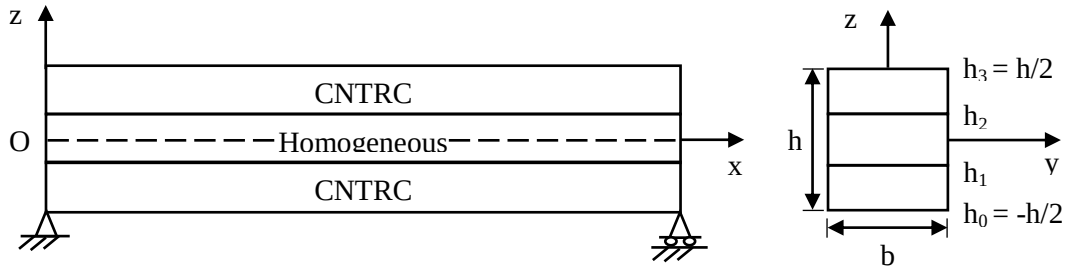


*Figure 1.* Geometry and coordinate system of sandwich beams

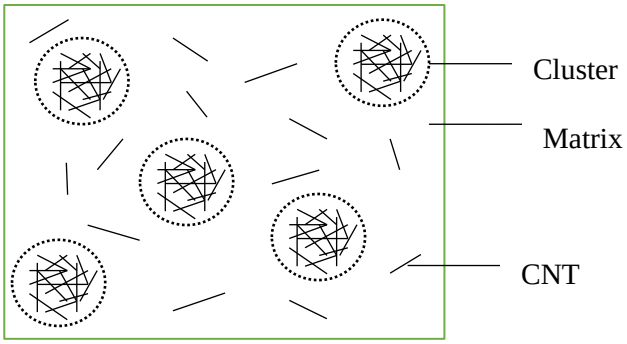


*Figure 2.* RVE with Eshelby cluster model of agglomeration of CNTs.

Denoted by $h_0 = -h/2, h_1, h_2, h_3 = h/2$ are, respectively, the vertical coordinates of the bottom surface, the interfaces between the layers and the top surface.

Figure 2 shows the representative volume element (RVE) $V$, in which there are some regions with a higher concentration CNTs, called spherical clusters. The total volume $V_r$ of CNTs in the RVE $V$ can be divided into the following two parts:

$$V_r = V_r^{cluster} + V_r^m \tag{1}$$

where $V_r^{cluster}$ and $V_r^m$ represent the volumes of CNTs inside and outside of the cluster (matrix), respectively. Two parameters are introduced to describe the agglomeration:

$$\xi = \frac{V_{cluster}}{V},\ \zeta = \frac{V_r^{cluster}}{V_r},\ 0 \le \xi, \zeta \le 1 \tag{2}$$

where $V_{cluster}$ is the volume of clusters in the RVE; $\xi$ denotes the volume fraction of clusters with respect to the total volume of the RVE, and $\zeta$ is the volume ratio of the CNTs inside the clusters over the total CNT inside the RVE. In special cases, $\xi = 1$, CNTs are uniformity distributed in the matrix, $\xi$ decreases leads to the agglomeration increases. When $\zeta = 1$, all CNTs are located in the clusters. The case $\xi = \zeta$ means that the volume fraction of CNTs inside the clusters is as same as that of CNTs outside the clusters. In the case $\zeta > \xi$, the value of $\zeta$ is bigger, the distribution of CNTs is more heterogeneous. The volume fraction $V_{CNT}$ of CNTs in the composite is $V_{CNT} = \frac{V_r}{V}$.

The effective bulk and shear moduli of the clusters $K_{in}$, $G_{in}$, and those of the region outside the clusters $K_{out}, G_{out}$ may be calculated by [6]:

$$\begin{aligned}
&K_{in} = K_m + \frac{V_{CNT}\zeta\left(\delta_r - 3K_m\alpha_r\right)}{3\left(\xi - V_{CNT}\zeta + V_{CNT}\zeta\alpha_r\right)};\quad G_{in} = G_m + \frac{V_{CNT}\zeta\left(\eta_r - 2G_m\beta_r\right)}{2\left(\xi - V_{CNT}\zeta + V_{CNT}\zeta\beta_r\right)};\\
&K_{out} = K_m + \frac{V_{CNT}\left(1-\zeta\right)\left(\delta_r - 3K_m\alpha_r\right)}{3\left[1-\xi - V_{CNT}\left(1-\zeta\right) + V_{CNT}\left(1-\zeta\right)\alpha_r\right]};\\
&G_{out} = G_m + \frac{V_{CNT}\left(1-\zeta\right)\left(\eta_r - 2G_m\beta_r\right)}{2\left[1-\xi - V_{CNT}\left(1-\zeta\right) + V_{CNT}\left(1-\zeta\right)\zeta\beta_r\right]}
\end{aligned} \tag{3}$$

with

$$\alpha_r = \frac{3\left(K_m + G_m\right) + k_r - l_r}{3\left(G_m + k_r\right)},\ \delta_r = \frac{1}{3}\left[ n_r + 2l_r + \frac{\left(2k_r + l_r\right)\left(3K_m + 2G_m - l_r\right)}{G_m + k_r} \right],$$

$$\beta_r = \frac{1}{5}\left( \frac{4G_m + 2k_r + l_r}{3\left(G_m + k_r\right)} + \frac{4G_m}{G_m + p_r} + \frac{2\left[ G_m\left(3K_m + G_m\right) + G_m\left(3K_m + 7G_m\right) \right]}{G_m\left(3K_m + G_m\right) + m_r\left(3K_m + 7G_m\right)} \right), \tag{4}$$

$$\eta_r = \frac{1}{5}\left[ \frac{2}{3}\left(n_r - l_r\right) + \frac{8G_m p_r}{G_m + p_r} + \frac{8m_r G_m\left(3K_m + 4G_m\right)}{3K_m\left(m_r + G_m\right) + G_m\left(7m_r + G_m\right)} + \frac{\left(2k_r - l_r\right)\left(2G_m + l_r\right)}{3\left(G_m + k_r\right)} \right]$$

where $K_m = \frac{E_m}{3\left(1-2\upsilon_m\right)}$ and $G_m = \frac{E_m}{2\left(1+\upsilon_m\right)}$ are the bulk and shear moduli of the matrix, respectively. In Eqs. (3) and (4), the subscripts *m* and *r* stand for the quantities of the matrix and the reinforcing phase; $k_r, l_r, m_r, n_r, p_r$ are the Hill's elastic moduli for the reinforcing phase.

The Mori-Tanaka scheme is adopted herein to estimate the effective properties of the composite. The bulk modulus *K* and the shear modulus *G* of the composite are calculated as [6]:

$$K = K_{out}\left( 1 + \frac{\xi\left( \frac{K_{in}}{K_{out}} - 1 \right)}{1 + \alpha\left(1-\xi\right)\left( \frac{K_{in}}{K_{out}} - 1 \right)} \right),\ G = G_{out}\left( 1 + \frac{\xi\left( \frac{G_{in}}{G_{out}} - 1 \right)}{1 + \beta\left(1-\xi\right)\left( \frac{G_{in}}{G_{out}} - 1 \right)} \right) \tag{5}$$

where $\alpha = \frac{1+\nu_{out}}{3\left(1-\nu_{out}\right)}$, $\beta = \frac{8-10\nu_{out}}{15\left(1-\nu_{out}\right)}$, $\nu_{out} = \frac{\left(3K_{out} - 2G_{out}\right)}{2\left(3K_{out} + G_{out}\right)}$. Noting that in the case CNTs are oriented completely at random throughout the matrix, the composite is considered to be isotropic. Then, bulk and shear moduli, *K* and *G*, are obtained by [6]:

$$K = K_m + \frac{V_{CNT}\left(\delta_r - 3K_m\alpha_r\right)}{3\left(c_m + V_{CNT}\alpha_r\right)},\ G = G_m + \frac{V_{CNT}\left(\eta_r - 2G_m\beta_r\right)}{2\left(c_m + V_{CNT}\beta_r\right)} \tag{6}$$

where $c_m = 1 - V_{CNT}$, and $\alpha_r, \delta_r, \beta_r, \eta_r$ as given in Eq. (4).

The effective Young's modulus *E* and Poisson's ratio $\nu$ of the composite can be derived by:

$$E = \frac{9KG}{3K + G};\ \nu = \frac{3K - 2G}{6K + 2G} \tag{7}$$

The equivalent density of the CNT reinforced layer can be formulated as [15]:

$$\rho = \left(\rho^{CNT} - \rho^m\right)V_{CNT} + \rho^m \tag{8}$$

## 3. MATHEMATICAL FORMULATION

Based on the trigonometric shear deformation theory [12], the displacements of a point in the *x* and *z* directions are, respectively, given by

$$u(x,z,t) = u_0(x,t) - zw_{0,x} + \sin\frac{\pi z}{h}\theta;\ \ w(x,z,t) = w_0(x,t) \tag{9}$$

where $u_0\left(x,t\right)$ and $w_0\left(x,t\right)$ are, respectively, the displacements in the *x* and *z* directions of a point on the *x*-axis; $\theta$ is the cross-sectional rotation, and *t* is the time variable.

The axial strain $\varepsilon_{xx}$ and shear strain $\gamma_{xz}$ resulting from Eq. (9) are

$$\varepsilon_{xx} = u_{0,x} - zw_{0,xx} + \sin\frac{\pi z}{h}\theta_{,x};\ \ \gamma_{xz} = \frac{\pi}{h}\cos\frac{\pi z}{h}\theta \tag{10}$$

Since the beam is made of three layers, the stress–strain relations in the $k^{th}$ layer are given as:

$$\sigma_{xx}^{(k)} = E^{(k)}\varepsilon_{xx};\ \tau_{xz}^{(k)} = G^{(k)}\gamma_{xz} \quad (k = 1,2,3) \tag{11}$$

The elastic strain energy of the sandwich beam $U$ is given by

$$\begin{aligned} U &= \frac{1}{2}\int_0^L\int_A (\sigma_{xx}^{(k)}\varepsilon_{xx} + \tau_{xz}^{(k)}\gamma_{xz})\, dAdx \\ &= \frac{1}{2}\int_0^L \left[ A_1 u_{0,x}^2 - 2A_2 u_{0,x}w_{0,xx} + 2A_3 u_{0,x}\theta_{,x} - 2A_4 w_{0,xx}\theta_{,x} + A_5\theta_{,x}^2 + A_6 w_{0,xx}^2 + A_7\theta^2 \right] dx \end{aligned} \tag{12}$$

where $A = bh$ is the cross-section area; $A_1, A_2, \ldots A_7$ are the beam rigidities, defined as

$$\begin{aligned} \left(A_1, A_2, A_3, A_4, A_5, A_6\right) &= b\int_{h_0}^{h_3} E\left(1,\ z,\ \sin\frac{\pi z}{h},\ z\sin\frac{\pi z}{h},\ \sin^2\frac{\pi z}{h},\ z^2\right)dz \\ &= b\sum_{k=1}^{3}\int_{h_{k-1}}^{h_k} E^{(k)}\left(1,\ z,\ \sin\frac{\pi z}{h},\ z\sin\frac{\pi z}{h},\ \sin^2\frac{\pi z}{h},\ z^2\right)dz; \\ A_7 &= b\frac{\pi^2}{h^2}\int_{h_0}^{h_3} G\cos^2\frac{\pi z}{h}dz = b\frac{\pi^2}{h^2}\sum_{k=1}^{3}\int_{h_{k-1}}^{h_k} G^{(k)}\cos^2\frac{\pi z}{h}dz \end{aligned} \tag{13}$$

The kinetic energy $T$ of the sandwich beam is given by

$$\begin{aligned} T &= \frac{1}{2}\int_0^L\int_A \rho\left(\dot{u}^2 + \dot{w}^2\right)dAdx \\ &= \frac{1}{2}\int_0^L \left[ I_1\left(\dot{u}_0^2 + \dot{w}_0^2\right) - 2I_2\dot{u}_0\dot{w}_{0,x} + 2I_3\dot{u}_0\dot{\theta} - 2I_4\dot{w}_{0,x}\dot{\theta} + I_5\dot{\theta}^2 + I_6\dot{w}_{0,x}^2 \right]dx \end{aligned} \tag{14}$$

where the over dot denotes the derivative with respect to time variable; $I_1, I_2, \ldots I_6$ are the mass moments, defined as

$$\begin{aligned} \left(I_1, I_2, I_3, I_4, I_5, I_6\right) &= b\int_{h_0}^{h_3} \rho\left(1,\ z,\ \sin\frac{\pi z}{h},\ z\sin\frac{\pi z}{h},\ \sin^2\frac{\pi z}{h},\ z^2\right)dz \\ &= b\sum_{k=1}^{3}\int_{h_{k-1}}^{h_k} \rho^{(k)}\left(1,\ z,\ \sin\frac{\pi z}{h},\ z\sin\frac{\pi z}{h},\ \sin^2\frac{\pi z}{h},\ z^2\right)dz \end{aligned} \tag{15}$$

## 4. FINITE ELEMENT FORMULATION

A two-node beam element with length $l$ is considered herewith. Linear functions are used to interpolate the axial displacement $u_0$ and cross-sectional rotation $\theta$, while cubic Hermite polynomials are used for the transverse displacement $w_0$ as

$$u_0 = \mathbf{N}\mathbf{d}_{u_0};\ w_0 = \mathbf{H}\mathbf{d}_{w_0};\ \theta = \mathbf{N}\mathbf{d}_{\theta} \tag{16}$$

where

$$\mathbf{d}_{u_0}=\{u_{01}\ u_{02}\}^T;\ \mathbf{d}_{w_0}=\{w_{01}\ w_{0x1}\ w_{02}\ w_{0x2}\}^T;\ \mathbf{d}_{\theta}=\{\theta_1\ \theta_2\}^T \tag{17}$$

are, respectively, the vectors of nodal displacement for $u_0, w_0$ and $\theta$ at nodes 1 and 2; $\mathbf{N}=\{N_0\ N_1\}$ and $\mathbf{H}=\{H_0\ H_1\ H_2\ H_3\}$ are the matrices of the linear and Hermite shape functions. To improve the efficiency of the beam element, Lagrange and Hermite interpolations are enriched herein by hierarchical functions. Four higher-order hierarchic polynomials are used herewith to enrich the original functions, and the interpolation (16) is now replaced by [13]

$$u_0=\mathbf{N}\mathbf{d}_{u_0}+\hat{\mathbf{N}}_5\hat{\mathbf{d}}_{u_0};\ w_0=\mathbf{H}\mathbf{d}_{w_0}+\hat{\mathbf{H}}_7\hat{\mathbf{d}}_{w_0};\ \theta=\mathbf{N}\mathbf{d}_{\theta}+\hat{\mathbf{N}}_5\hat{\mathbf{d}}_{\theta} \tag{18}$$

where $\hat{\mathbf{N}}_5=\{N_2\ N_3\ N_4\ N_5\}$ and $\hat{\mathbf{H}}_7=\{H_4\ H_5\ H_6\ H_7\}$ are matrices of the enriched shape functions; $\hat{\mathbf{d}}_{u_0}, \hat{\mathbf{d}}_{w_0}$ and $\hat{\mathbf{d}}_{\theta}$ are the supplemented vectors of unknowns with the following forms

$$\hat{\mathbf{d}}_{u_0}=\{\hat{u}_1\ \hat{u}_2\ \hat{u}_3\ \hat{u}_4\}^T,\ \hat{\mathbf{d}}_{w_0}=\{\hat{w}_1\ \hat{w}_2\ \hat{w}_3\ \hat{w}_4\}^T,\ \hat{\mathbf{d}}_{\theta}=\{\hat{\theta}_1\ \hat{\theta}_2\ \hat{\theta}_3\ \hat{\theta}_4\}^T \tag{19}$$

The enrichment functions $N_i\ (i=2\ldots5)$ and $H_j\ (j=4\ldots7)$, derived in [13,14] are given below

$$\begin{aligned}&N_2=\sqrt{6}\frac{x}{l}\left(\frac{x}{l}-1\right),\ N_3=\sqrt{10}\frac{x}{l}\left(\frac{x}{l}-1\right)\left(\frac{2x}{l}-1\right),\\&N_4=\sqrt{14}\frac{x}{l}\left(\frac{x}{l}-1\right)\left(\frac{5x^2}{l^2}-\frac{5x}{l}+1\right),\ N_5=\sqrt{18}\frac{x}{l}\left(\frac{x}{l}-1\right)\left(\frac{7x^2}{l^2}-\frac{7x}{l}+1\right)\left(\frac{2x}{l}-1\right)\end{aligned} \tag{20}$$

and

$$\begin{aligned}&H_4=\sqrt{10}\frac{x^2}{l^2}\left(1-\frac{x}{l}\right)^2,\ H_5=\sqrt{14}\frac{x^2}{l^2}\left(1-\frac{x}{l}\right)^2\left(\frac{2x}{l}-1\right),\\&H_6=\sqrt{2}\frac{x^2}{l^2}\left(1-\frac{x}{l}\right)^2\left(-\frac{14x^2}{l^2}+\frac{14x}{l}-3\right),\ H_7=\sqrt{22}\frac{x^2}{l^2}\left(1-\frac{x}{l}\right)^2\left(\frac{6x^2}{l^2}-\frac{6x}{l}+1\right)\left(\frac{2x}{l}-1\right)\end{aligned} \tag{21}$$

With the enriched interpolations, the vector of degrees of freedom for the element $(\mathbf{d})$ contains 20 components, and it can be written as

$$\underset{20\times1}{\mathbf{d}}=\{\mathbf{d}_{u_0}\ \hat{\mathbf{d}}_{u_0}\ \mathbf{d}_{w_0}\ \hat{\mathbf{d}}_{w_0}\ \mathbf{d}_{\theta}\ \hat{\mathbf{d}}_{\theta}\}^T \tag{22}$$

where $\mathbf{d}_{u_0}, \mathbf{d}_{w_0}, \mathbf{d}_{\theta}$ are given by Eq. (17), and $\hat{\mathbf{d}}_{u_0}, \hat{\mathbf{d}}_{w_0}, \hat{\mathbf{d}}_{\theta}$ are defined by (19). Using Eqs. (18) and (22), one can write the strain energy in Eq. (12) in the following matrix form

$$U=\frac{1}{2}\sum_{i=1}^{ne}\mathbf{d}_i^T\mathbf{k}_i\,\mathbf{d}_i \tag{23}$$

where *ne* is the total number of elements used to discrete the beam, and **k** is the element stiffness matrix, which can be split into sub-matrices as

$$\underset{20\times20}{\mathbf{k}}=\begin{bmatrix}\mathbf{k}_{u_0u_0} & \mathbf{k}_{u_0\hat{u}_0} & \mathbf{k}_{u_0w_0} & \mathbf{k}_{u_0\hat{w}_0} & \mathbf{k}_{u_0\theta} & \mathbf{k}_{u_0\hat{\theta}}\\ \mathbf{k}^T_{u_0\hat{u}_0} & \mathbf{k}_{\hat{u}_0\hat{u}_0} & \mathbf{k}_{\hat{u}_0w_0} & \mathbf{k}_{\hat{u}_0\hat{w}_0} & \mathbf{k}_{\hat{u}_0\theta} & \mathbf{k}_{\hat{u}_0\hat{\theta}}\\ \mathbf{k}^T_{u_0w_0} & \mathbf{k}^T_{\hat{u}_0w_0} & \mathbf{k}_{w_0w_0} & \mathbf{k}_{w_0\hat{w}_0} & \mathbf{k}_{w_0\theta} & \mathbf{k}_{w_0\hat{\theta}}\\ \mathbf{k}^T_{u_0\hat{w}_0} & \mathbf{k}^T_{\hat{u}_0\hat{w}_0} & \mathbf{k}^T_{w_0\hat{w}_0} & \mathbf{k}_{\hat{w}_0\hat{w}_0} & \mathbf{k}_{\hat{w}_0\theta} & \mathbf{k}_{\hat{w}_0\hat{\theta}}\\ \mathbf{k}^T_{u_0\theta} & \mathbf{k}^T_{\hat{u}_0\theta} & \mathbf{k}^T_{w_0\theta} & \mathbf{k}^T_{\hat{w}_0\theta} & \mathbf{k}_{\theta\theta} & \mathbf{k}_{\theta\hat{\theta}}\\ \mathbf{k}^T_{u_0\hat{\theta}} & \mathbf{k}^T_{\hat{u}_0\hat{\theta}} & \mathbf{k}^T_{w_0\hat{\theta}} & \mathbf{k}^T_{\hat{w}_0\hat{\theta}} & \mathbf{k}^T_{\theta\hat{\theta}} & \mathbf{k}_{\hat{\theta}\hat{\theta}}\end{bmatrix} \tag{24}$$

The sub-matrices in the diagonal of the above element stiffness matrix have the following forms

$$\begin{aligned}
&\underset{2\times2}{\mathbf{k}_{u_0u_0}}=\int_0^l\mathbf{N}^T_{,x}A_1\mathbf{N}_{,x}dx,\ \underset{4\times4}{\mathbf{k}_{\hat{u}_0\hat{u}_0}}=\int_0^l\hat{\mathbf{N}}^T_{5,x}A_1\hat{\mathbf{N}}_{5,x}dx,\\
&\underset{4\times4}{\mathbf{k}_{w_0w_0}}=\int_0^l\mathbf{H}^T_{,xx}A_6\mathbf{H}_{,xx}dx,\ \underset{4\times4}{\mathbf{k}_{\hat{w}_0\hat{w}_0}}=\int_0^l\hat{\mathbf{H}}^T_{7,xx}A_6\hat{\mathbf{H}}_{7,xx}dx\\
&\underset{2\times2}{\mathbf{k}_{\theta\theta}}=\int_0^l\left(\mathbf{N}^T_{,x}A_5\mathbf{N}_{,x}+\mathbf{N}^TA_7\mathbf{N}\right)dx,\underset{4\times4}{\mathbf{k}_{\hat{\theta}\hat{\theta}}}=\int_0^l\left(\hat{\mathbf{N}}^T_{5,x}A_5\hat{\mathbf{N}}_{5,x}+\hat{\mathbf{N}}^T_5A_7\hat{\mathbf{N}}_5\right)dx,
\end{aligned} \tag{25}$$

and the off-diagonal sub-matrices are

$$\begin{aligned}
&\underset{2\times4}{\mathbf{k}_{u_0\hat{u}_0}}=\int_0^l\mathbf{N}^T_{,x}A_1\hat{\mathbf{N}}_{5,x}dx,\ \underset{2\times4}{\mathbf{k}_{u_0w_0}}=-\int_0^l\mathbf{N}^T_{,x}A_2\mathbf{H}_{,xx}dx,\ \underset{2\times4}{\mathbf{k}_{u_0\hat{w}_0}}=-\int_0^l\mathbf{N}^T_{,x}A_2\hat{\mathbf{H}}_{7,xx}dx,\ \underset{2\times2}{\mathbf{k}_{u_0\theta}}=\int_0^l\mathbf{N}^T_{,x}A_3\mathbf{N}_{,x}dx\\
&\underset{2\times4}{\mathbf{k}_{u_0\hat{\theta}}}=\int_0^l\mathbf{N}^T_{,x}A_3\hat{\mathbf{N}}_{5,x}dx,\ \underset{4\times4}{\mathbf{k}_{\hat{u}_0w_0}}=-\int_0^l\hat{\mathbf{N}}^T_{5,x}A_2\mathbf{H}_{,xx}dx,\ \underset{4\times4}{\mathbf{k}_{\hat{u}_0\hat{w}_0}}=-\int_0^l\hat{\mathbf{N}}^T_{5,x}A_2\hat{\mathbf{H}}_{7,xx}dx,\underset{4\times2}{\mathbf{k}_{\hat{u}_0\theta}}=\int_0^l\hat{\mathbf{N}}^T_{5,x}A_3\mathbf{N}_{,x}dx\\
&\underset{4\times4}{\mathbf{k}_{\hat{u}_0\hat{\theta}}}=\int_0^l\hat{\mathbf{N}}^T_{5,x}A_3\hat{\mathbf{N}}_{5,x}dx,\ \underset{4\times4}{\mathbf{k}_{w_0\hat{w}_0}}=\int_0^l\mathbf{H}^T_{,xx}A_6\hat{\mathbf{H}}_{7,xx}dx,\underset{4\times2}{\mathbf{k}_{w_0\theta}}=-\int_0^l\mathbf{H}^T_{,xx}A_4\mathbf{N}_{,x}dx,\underset{4\times4}{\mathbf{k}_{w_0\hat{\theta}}}=-\int_0^l\mathbf{H}^T_{,xx}A_4\hat{\mathbf{N}}_{5,x}dx\\
&\underset{4\times2}{\mathbf{k}_{\hat{w}_0\theta}}=-\int_0^l\hat{\mathbf{H}}^T_{7,xx}A_4\mathbf{N}_{,x}dx,\ \underset{4\times4}{\mathbf{k}_{w_0\hat{\theta}}}=-\int_0^l\mathbf{H}^T_{,xx}A_4\hat{\mathbf{N}}_{5,x}dx,\ \underset{2\times4}{\mathbf{k}_{\theta\hat{\theta}}}=\int_0^l\left(\mathbf{N}^T_{,x}A_5\hat{\mathbf{N}}_{5,x}+\mathbf{N}^TA_7\hat{\mathbf{N}}_5\right)dx
\end{aligned} \tag{26}$$

Similarly, the kinetic energy $T$ in Eq. (14) can also be written in the following matrix form as

$$T=\frac{1}{2}\sum_{i=1}^{ne}\dot{\mathbf{d}}_i^T\mathbf{m}_i\,\dot{\mathbf{d}}_i \tag{27}$$

with the element mass matrix of the beam $\mathbf{m}$ can be written in sub-matrices as

$$\underset{20\times20}{\mathbf{m}}=\begin{bmatrix}\mathbf{m}_{u_0u_0} & \mathbf{m}_{u_0\hat{u}_0} & \mathbf{m}_{u_0w_0} & \mathbf{m}_{u_0\hat{w}_0} & \mathbf{m}_{u_0\theta} & \mathbf{m}_{u_0\hat{\theta}}\\ \mathbf{m}^T_{u_0\hat{u}_0} & \mathbf{m}_{\hat{u}_0\hat{u}_0} & \mathbf{m}_{\hat{u}_0w_0} & \mathbf{m}_{\hat{u}_0\hat{w}_0} & \mathbf{m}_{\hat{u}_0\theta} & \mathbf{m}_{\hat{u}_0\hat{\theta}}\\ \mathbf{m}^T_{u_0w_0} & \mathbf{m}^T_{\hat{u}_0w_0} & \mathbf{m}_{w_0w_0} & \mathbf{m}_{w_0\hat{w}_0} & \mathbf{m}_{w_0\theta} & \mathbf{m}_{w_0\hat{\theta}}\\ \mathbf{m}^T_{u_0\hat{w}_0} & \mathbf{m}^T_{\hat{u}_0\hat{w}_0} & \mathbf{m}^T_{w_0\hat{w}_0} & \mathbf{m}_{\hat{w}_0\hat{w}_0} & \mathbf{m}_{\hat{w}_0\theta} & \mathbf{m}_{\hat{w}_0\hat{\theta}}\\ \mathbf{m}^T_{u_0\theta} & \mathbf{m}^T_{\hat{u}_0\theta} & \mathbf{m}^T_{w_0\theta} & \mathbf{m}^T_{\hat{w}_0\theta} & \mathbf{m}_{\theta\theta} & \mathbf{m}_{\theta\hat{\theta}}\\ \mathbf{m}^T_{u_0\hat{\theta}} & \mathbf{m}^T_{\hat{u}_0\hat{\theta}} & \mathbf{m}^T_{w_0\hat{\theta}} & \mathbf{m}^T_{\hat{w}_0\hat{\theta}} & \mathbf{m}^T_{\theta\hat{\theta}} & \mathbf{m}_{\hat{\theta}\hat{\theta}}\end{bmatrix} \tag{28}$$

in which

$$\mathbf{m}_{\underset{2\times2}{u_0u_0}}=\int_0^l \mathbf{N}^T I_1\mathbf{N}dx,\ \mathbf{m}_{\underset{4\times4}{\hat{u}_0\hat{u}_0}}=\int_0^l \hat{\mathbf{N}}_5^T I_1\hat{\mathbf{N}}_5 dx$$
$$\mathbf{m}_{\underset{4\times4}{w_0w_0}}=\int_0^l \left(\mathbf{H}^T I_1\mathbf{H}+\mathbf{H}_{,x}^T I_6\mathbf{H}_{,x}\right)dx,\ \mathbf{m}_{\underset{4\times4}{\hat{w}_0\hat{w}_0}}=\int_0^l \left(\mathbf{H}_7^T I_1\mathbf{H}_7+\mathbf{H}_{7,x}^T I_6\mathbf{H}_{7,x}\right)dx \tag{29}$$
$$\mathbf{m}_{\underset{2\times2}{\theta\theta}}=\int_0^l \mathbf{N}^T I_5\mathbf{N}dx,\mathbf{m}_{\underset{4\times4}{\hat{\theta}\hat{\theta}}}=\int_0^l \hat{\mathbf{N}}_5^T I_5\hat{\mathbf{N}}_5\, dx$$

and

$$\mathbf{m}_{\underset{2\times4}{u_0\hat{u}_0}}=\int_0^l \mathbf{N}^T I_1\hat{\mathbf{N}}_5 dx,\ \mathbf{m}_{\underset{2\times4}{u_0w_0}}=-\int_0^l \mathbf{N}^T I_2\mathbf{H}_{,x}dx,\ \mathbf{m}_{\underset{2\times4}{u_0\hat{w}_0}}=-\int_0^l \mathbf{N}^T I_2\hat{\mathbf{H}}_{7,x}dx,\ \mathbf{m}_{\underset{2\times2}{u_0\theta}}=\int_0^l \mathbf{N}^T I_3\mathbf{N}dx$$
$$\mathbf{m}_{\underset{2\times4}{u_0\hat{\theta}}}=\int_0^l \mathbf{N}^T I_3\hat{\mathbf{N}}_5 dx,\ \mathbf{m}_{\underset{4\times4}{\hat{u}_0w_0}}=-\int_0^l \hat{\mathbf{N}}_5^T I_2\mathbf{H}_{,x}dx,\ \mathbf{m}_{\underset{4\times4}{\hat{u}_0\hat{w}_0}}=-\int_0^l \hat{\mathbf{N}}_5^T I_2\hat{\mathbf{H}}_{7,x}dx,\mathbf{m}_{\underset{4\times2}{\hat{u}_0\theta}}=\int_0^l \hat{\mathbf{N}}_5^T I_3\mathbf{N}dx$$
$$\mathbf{m}_{\underset{4\times4}{\hat{u}_0\hat{\theta}}}=\int_0^l \hat{\mathbf{N}}_5^T I_3\hat{\mathbf{N}}_5 dx,\ \mathbf{m}_{\underset{4\times4}{w_0\hat{w}_0}}=\int_0^l \left(\mathbf{H}^T I_1\hat{\mathbf{H}}_7+\mathbf{H}_{,x}^T I_6\hat{\mathbf{H}}_{7,x}\right)dx,\mathbf{m}_{\underset{4\times2}{w_0\theta}}=-\int_0^l \mathbf{H}_{,x}^T I_4\mathbf{N}dx \tag{30}$$
$$\mathbf{m}_{\underset{4\times4}{w_0\hat{\theta}}}=-\int_0^l \mathbf{H}_{,x}^T I_4\hat{\mathbf{N}}_5 dx,\ \mathbf{m}_{\underset{4\times2}{\hat{w}_0\theta}}=-\int_0^l \hat{\mathbf{H}}_{7,x}^T I_4\mathbf{N}dx,\ \mathbf{m}_{\underset{4\times4}{w_0\hat{\theta}}}=-\int_0^l \mathbf{H}_{,x}^T I_4\hat{\mathbf{N}}_5 dx,\ \mathbf{m}_{\underset{2\times4}{\theta\hat{\theta}}}=\int_0^l \mathbf{N}^T I_5\hat{\mathbf{N}}_5\, dx$$

Using the derived stiffness and mass matrices, the equations of motion for the free vibration analysis can be written in the form

$$\mathbf{M}\ddot{\mathbf{D}}+\mathbf{K}\mathbf{D}=\mathbf{0} \tag{31}$$

where **D**, **M** and **K** are the global nodal displacement vector, mass and stiffness matrices, obtained by assembling the corresponding element vector and matrices over the total elements, respectively. Assuming a harmonic response for the free vibration, Eq. (31) leads to

$$\left(\mathbf{K}-\omega^2\mathbf{M}\right)\bar{\mathbf{D}}=\mathbf{0} \tag{32}$$

with $\omega$ is the circular frequency, and $\bar{\mathbf{D}}$ is the vibration amplitude. Eq. (32) leads to an eigenvalue problem, which can be solved by the standard method.

## 5. NUMERICAL RESULTS AND DISCUSSION

Numerical results on free vibration of the sandwich beam are presented in this section. The material properties of the matrix are as follows [15]: $E_m=10\,\text{GPa}$, $\rho_m=1150\,\text{kg/m}^3$, $\nu_m=0.3$; the armchair (10,10) SWCNTs are used as the reinforcements with $\rho^{CNT}=1400\,\text{kg/m}^3$. The material in matrix is chosen as the core material of the sandwich beam.

A simply supported sandwich beam with $L/h=20$, $b=0.4\,\text{m}$, $h=1\,\text{m}$ is considered. Three numbers in parentheses, e.g. (2-1-1), are used below to denote the layer thickness ratio of the beam layers, from the bottom layer to the top layer. The fundamental frequency parameter is defined as $\mu=\omega\dfrac{L^2}{h}\sqrt{\dfrac{\rho_m}{E_m}}$ where $\omega$ is the fundamental natural frequency.

### 5.1. Formulation verification

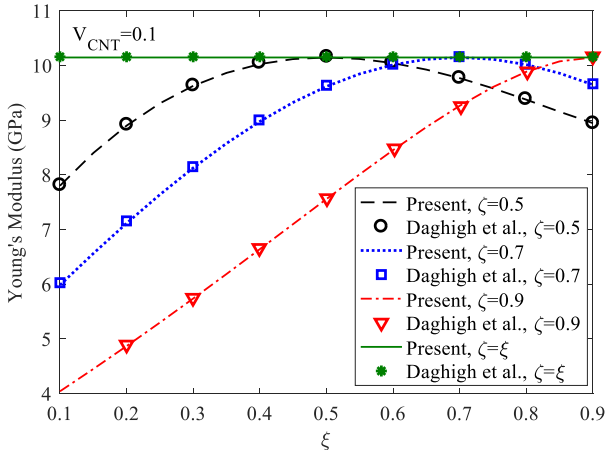


*Figure 3.* Comparison of Young's modulus for $V_{CNT} = 0.1$ and different agglomeration parameters.

In order to examine the accuracy and reliability of the present study, the effective Young's modulus of an agglomerated randomly oriented CNTRC beam obtained herein are compared with that of Daghigh *et al.* [15] in Figure 3. The effect of agglomeration parameters $\zeta$ and $\xi$ on the Young's modulus is displayed in the figure. The Young's modulus for material in matrix phase is $E_m = 2.5\text{GPa}$; Hill's elastic modulus for the CNTs are taken form Ref. [6]. The elastic modulus curves in Figure 3 are plotted with the volume fraction of CNTs $V_{CNT} = 0.1$. A good agreement between Young's modulus of the present work with that of Daghigh *et al.* [15] is seen from Figure 3. Figure 3 also shows that the agglomeration parameters have a significant effect on the Young's modulus. Specifically, the effective Young's modulus increases with the increase of $\xi$, its approach the highest magnitude at $\zeta = \xi$ (fully dispersed), and then Young's modulus decreases.

*Table 1.* Convergence of enriched beam element in evaluating fundamental frequency parameters of beam reinforced with randomly oriented CNTs for different boundary conditions.

| Boundary conditions | Present | | | | | | Yas and Heshmati [16] | Error (%) |
|---|---|---|---|---|---|---|---|---|
| | ne = 1 | ne = 2 | ne = 4 | ne = 6 | ne = 8 | ne = 10 | | |
| CC | 5.1531 | 5.1517 | 5.1507 | 5.1505 | 5.1503 | 5.1501 | 5.098585 | 1 % |
| CS | 4.2914 | 4.2908 | 4.2905 | 4.2904 | 4.2904 | 4.2904 | 4.356794 | 1.55 % |
| CF | 2.0570 | 2.0569 | 2.0569 | 2.0569 | 2.0569 | 2.0569 | 2.151246 | 4.59 % |
| SS | 3.4423 | 3.4423 | 3.4423 | 3.4423 | 3.4423 | 3.4423 | 3.574603 | 3.84 % |

Table 1 lists the fundamental frequency parameters of a randomly oriented CNTRC beam with $V_{CNT} = 0.075$ predicted by different numbers of the enriched elements. The result obtained by 100 Timoshenko beam elements in [16] is also given in the table. The frequency parameter defined as in [16] is $\lambda^2 = \omega L^2 \sqrt{\rho_m A / E_m I}$ where $I = bh^3/12$. The table shows a fast convergence of the present element, and the convergence can be achieved by just one element for SS beam, two elements for CF beam, six elements for CS beam, and ten elements for CC beam. It can be seen that there is a difference in the frequency parameters obtained herein with

that of Ref. [16], but this error is still acceptable. Noting that Ref. [16] ignored the CNT agglomeration effect.

### 5.2. Natural frequencies

Figure 4 shows the variation of the frequency parameters with the agglomeration parameter $\zeta$ for various thickness ratios. Two values of agglomeration parameter $\xi$ are chosen to plot the figure $\xi = 0.2$, $\xi = 0.5$ and the volume of CNTs is $V_{CNT} = 0.1$. It is worth to note from Figure 4 that the layer thickness ratio and agglomeration parameters significantly affect the frequency parameters of the sandwich beam. More over, the increase of the core thickness results in a decrease in the frequency parameter. This also means that as the thickness of the face sheets increases leads to is an increase in the beam stiffness. The dependence of the frequency parameter upon the layer thickness ratio is influenced by the agglomeration parameters. The frequency parameter curves in Figure 4 will be closer when the parameter $\zeta$ is larger. This is more visible when the value of $\xi$ is smaller, as shown in Figure 4(a). The results in Figure 4 indicate that the highest frequency parameter is attained at $\zeta = \xi$, as the cases $\zeta = \xi = 0.2$ in Figure 4(a) and $\zeta = \xi = 0.5$ in Figure 4(b), while the lowest value occurs where the largest difference exists between the two agglomeration parameters, as shown in Figure 4(a) when $\xi = 0.2$ and $\zeta = 1$.

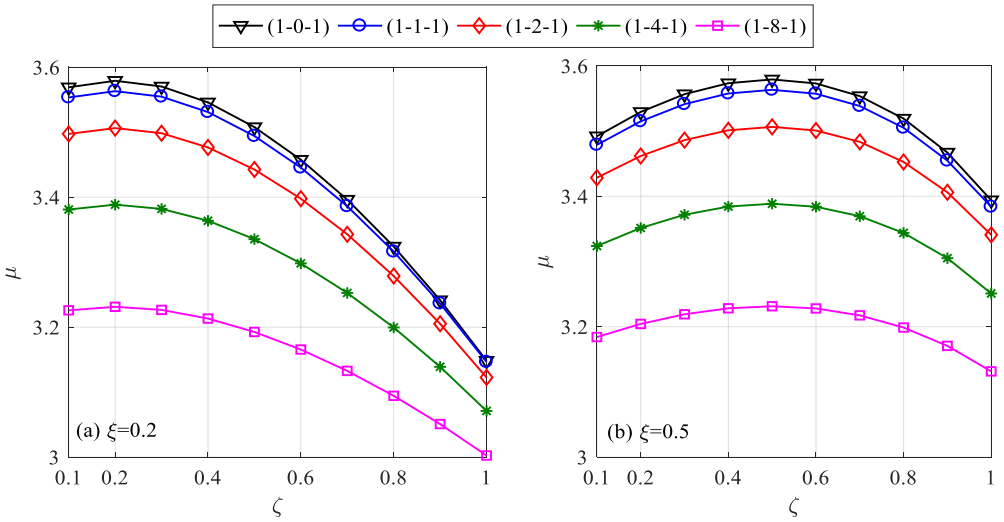


*Figure 4.* Fundamental frequency parameter of sandwich beam at $\xi = 0.2$ and $\xi = 0.5$, $V_{CNT} = 0.1$.

*Table 2.* Fundamental frequency parameters of (1-2-1) and (2-1-2) beams.

| | $\zeta = 1$ | $V_{CNT} = 0$ | $V_{CNT} = 0.02$ | $V_{CNT} = 0.05$ | $V_{CNT} = 0.1$ | $V_{CNT} = 0.2$ | $V_{CNT} = 0.3$ |
|---|---|---|---|---|---|---|---|
| (1-2-1) | $\xi = 0.1$ | 2.8372 | 2.9295 | 2.9767 | 3.0014 | 3.0078 | 3.0006 |
| | $\xi = 0.5$ | 2.8372 | 2.9801 | 3.1471 | 3.3448 | 3.5805 | 3.7122 |
| | $\xi = 1$ | 2.8372 | 2.9904 | 3.2009 | 3.5106 | 4.0206 | 4.4307 |
| (2-1-2) | $\xi = 0.1$ | 2.8372 | 2.9403 | 2.9914 | 3.0154 | 3.0151 | 2.9998 |
| | $\xi = 0.5$ | 2.8372 | 2.9975 | 3.1830 | 3.3995 | 3.6513 | 3.7865 |
| | $\xi = 1$ | 2.8372 | 3.0092 | 3.2433 | 3.5837 | 4.1353 | 4.5711 |

Table 2 shows the frequency parameters of (1-2-1) and (2-1-2) beams for different values of the parameter $\xi$ and the CNTs volume fraction $V_{CNT}$. For CNTRC beams, an increase in agglomeration parameter $\xi$ means that the agglomeration of CNTs decreases, leading to an increase in frequency parameter, regardless of the thickness ratio. In case of no agglomeration (fully dispersed CNTs), as $\zeta = \xi = 1$ in Table 2, the frequency parameter is the highest. As expected, an increase of the $V_{CNT}$ results in an increase of the frequency parameter, especially for beams reinforced with fully dispersed CNTs. However, looking more closely at Table 2, one can see that for the case of severe CNT agglomeration $(\xi = 0.1)$, the increase of the CNT volume fraction has a negative influence on the frequencies, namely the frequencies are decreased when increase the CNT volume fraction, especially for the beam associated with thicker face sheets. This phenomenon has also been pointed out by Kamarian *et al*. [10] in their vibration analysis of non-uniform piezoelectric sandwich beams.

The effect of the CNTs volume fraction on the frequency parameter of (1-2-1) and (2-1-2) beams is once again illustrated in Figure 5 corresponding to the agglomeration parameter $\xi = 0.2$. An increase of the CNTs volume fraction results in an increase of the frequency parameter. Furthermore, the increase in the CNTs volume fraction $V_{CNT}$ also affects the dependence of frequency parameter $\mu$ on agglomeration parameter $\zeta$. The influence of the parameter $\zeta$ on the parameter $\mu$ becomes even more pronounced for an increasing number of CNTs. Besides, it is easy to see from the Figure 5 that the CNTs volume fraction is more effective on the vibration behaviour of the CNTRC sandwich beams when the value of two agglomeration parameters gets close to each other. Opposite, as a discrepancy between $\xi$ and $\zeta$ leads to a decrease in the effect of CNTs volume fraction on the fundamental frequencies. Thus, in case of severe agglomeration ($\xi = 0.2$), the use of many CNTs does not significantly improve the vibration behaviour of the beam. All of these phenomena can be seen more clearly for beams with thicker face sheets, as shown in Figure 5(b).

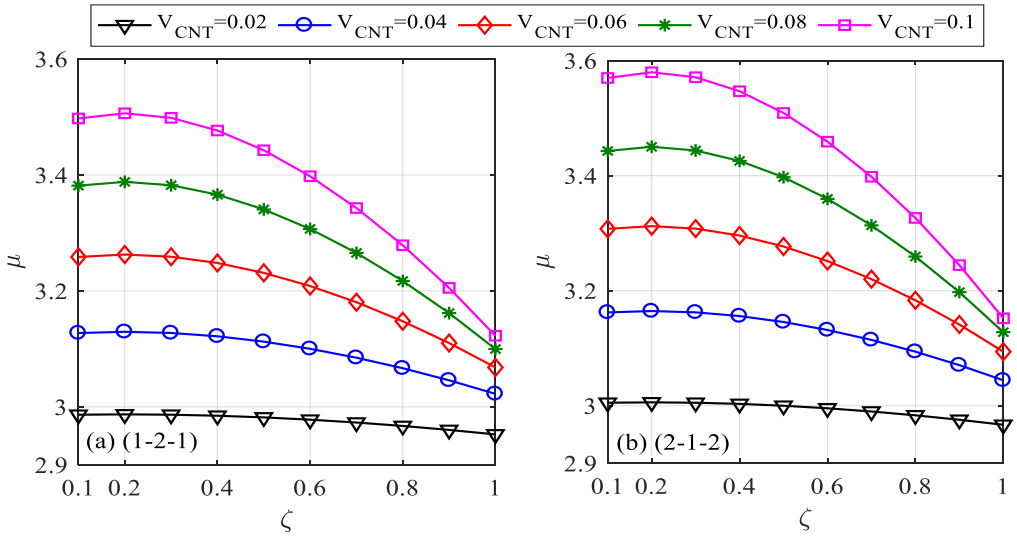


*Figure 5.* Fundamental frequency parameter of (1-2-1) and (2-1-2) beams at $\xi = 0.2$.

Similar conclusions can be achieved from Figures 4, 5 and Table 3, Figure 6 also illustrates that an increase in the CNTs volume fraction leads to a sharp increase in the frequency parameter, which happens when the agglomeration is not much. Further, the effect of the layer thickness ratio on the frequency parameter of the beam is also more visible when the agglomeration is reduced, the beams with thicker face sheets will have a higher frequency parameter.

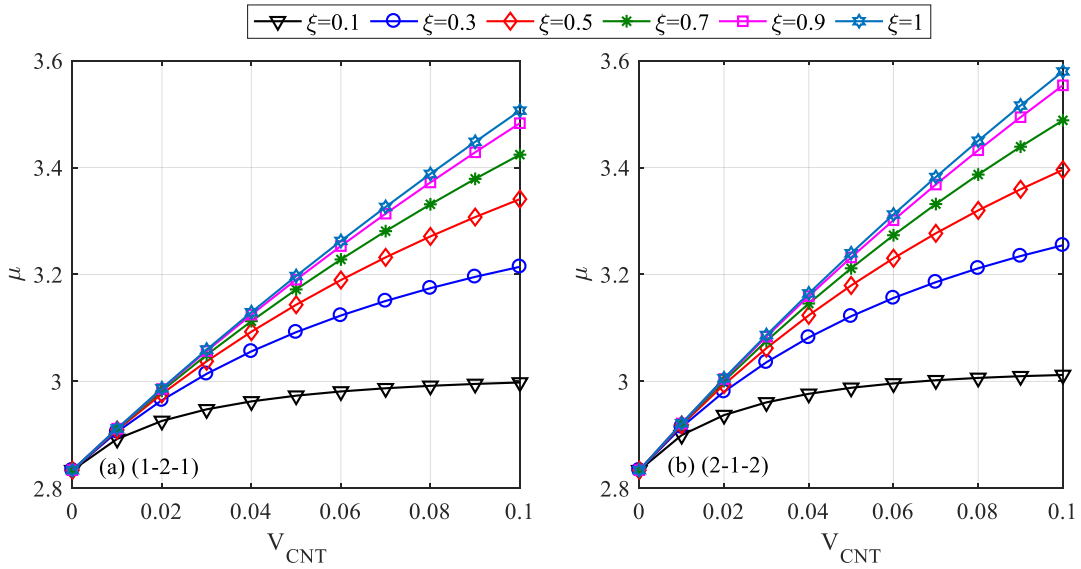


*Figure 6.* Fundamental frequency parameter of (1-2-1) and (2-1-2) beams at $\zeta = 1$.

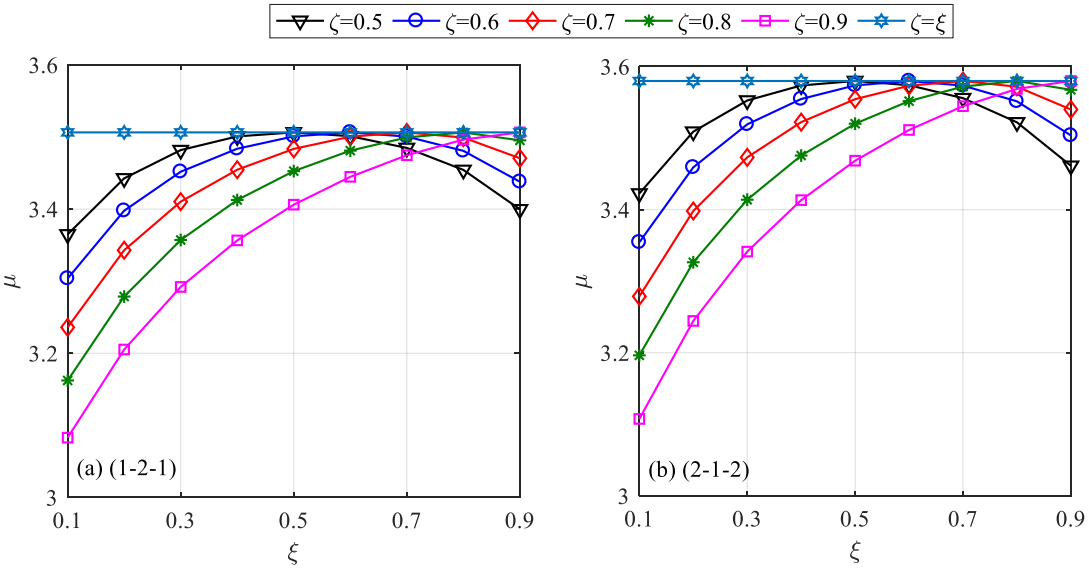


*Figure 7.* Fundamental frequency parameter of (1-2-1) and (2-1-2) beams at $V_{CNT} = 0.1$

The influence of two agglomeration parameters on the frequency parameters of (1-2-1) and (2-1-2) beams is again clearly seen in Figure 7. It is found that the frequency parameter curve behavior in Figure 7 is similar to that of the Young's modulus curve as shown in Figure 3. That is, the frequency parameter of the beam increases with the increase of agglomeration parameter $\xi$, the parameter $\mu$ reaches its maximum value at $\zeta = \xi$, and then gradually decreases.

## 6. CONCLUSIONS

The free vibration analysis of the agglomerated CNTRC sandwich beams considering the effect of CNT agglomeration was studied using an efficient finite beam element. The beam consists of a homogeneous core and two CNTRC face sheets. The Eshelby-Mori–Tanaka approach was employed to derive the effective material properties of the sandwich beams. The element is derived by using the hierarchic functions to enrich the conventional Lagrange and Hermite interpolations. Numerical investigation reveals that the enriched beam element is super convergent in evaluating the frequency parameters of the sandwich beams. The effects of the layer thickness ratio, agglomeration parameters and CNTs volume fraction on vibration behaviour of the sandwich beams have been examined in detail. Results presented the fact that free vibrations of CNTRC sandwich beams are seriously affected by CNTs agglomeration. The use of more reinforced CNTs as well as increasing the thickness of the face sheets will no longer be useful when CNTs agglomeration becomes severe.

***Acknowledgements.*** This research was made possible by the Grants "Phân tích động lực học dầm composite sandwich nghiêng chịu khối lượng di động bằng phần tử hữu hạn với hàm nội suy làm giàu", grant number CSCL03.02/22-23, Institute of Mechanics, Vietnam Academy of Science and Technology (Viet Nam).

***Authors contributions:*** Thi Thom Tran: validation, formal analysis, writing draft. Thi Thu Hoai Bui: software. Dinh Kien Nguyen: review and editing.

***Declaration of competing interest.*** We declare that we have no known competing financial interests or personal relationships that could have appeared to influence the work reported in this paper.

## REFERENCES

1. Ke L. L., Yang J. and Kitipornchai S. - Nonlinear free vibration of functionally graded carbon nanotubereinforced composite beams, Compos. Struct. **92** (2010) 676-683.
2. Yas M. H. and Samadi N. - Free vibrations and buckling analysis of carbon nanotubereinforced composite Timoshenko beams on elastic foundation, Int. J. Pressure Vessels Pip. **98** (2012) 119-128.
3. Lin F. and Xiang Y. - Vibration of carbon nanotube reinforced composite beams based on the first and third order beam theories, Appl. Math. Model **38** (2014) 3741-3754.
4. Ebrahimi F. and Farazmandnia N. - Thermo-mechanical vibration analysis of sandwich beams with functionally graded carbon nanotube-reinforced composite face sheets based on a higher-order shear deformation beam theory, Mech. Adv. Mater. Struct. **24** (2017). https://doi.org/10.1080/15376494.2016.1196786.
5. Mohseni A. and Shakouri M. - Vibration and stability analysis of functionally graded CNT-reinforced composite beams with variable thickness on elastic foundation, Proc. IMechE. Part L: J. Materials: Design and Applications **233** (2) (2019) 1-12.

6. Shi D. L., Feng X. Q., Huang Y. Y., Hwang K. C. and Gao H. - The effect of nanotube waviness and agglomeration on the elastic property of carbon nanotube reinforced composites, J. Eng. Mater. Technol**. 126** (2004) 250-257.
7. Heshmati M. and Yas M. H. - Free vibration analysis of functionally graded CNT-reinforced nanocomposite beam using Eshelby-Mori-Tanaka approach, J. Mech. Sci and Tech. **27**(11) (2013) 3403-3408.
8. Nejati M. and Eslampanah A. - Buckling and Vibration Analysis of Functionally Graded Carbon Nanotube-Reinforced Beam Under Axial Load, Int. J. Appl. Mech. **8** (1) (2016) 1650008. DOI: 10.1142/S1758825116500083.
9. Kamarian S., Shakeri M., Yas M.H., Bodaghi M. and Pourasghar A. - Free vibration analysis of functionally graded nanocomposite sandwich beams resting on Pasternak foundation by considering the agglomeration effect of CNTs, J. Sandwich Struct. Mater. **17** (6) (2015). DOI: 10.1177/1099636215590280.
10. Kamarian S., Bodaghi M., Pourasghar A. and Talebi S. - Vibrational Behavior of Non-Uniform Piezoelectric Sandwich Beams Made of CNT-Reinforced Polymer Nanocomposite by Considering the Agglomeration Effect of CNTs, Polym. Compos. **38** (S1) (2017) E553-E562.
11. Kiani F., Ariaseresht Y., Niroumand A. and Afshari H. - Thermo-mechanical buckling analysis of thick beams reinforced with agglomerated CNTs with temperature-dependent thermo-mechanical properties under a nonuniform thermal loading, Mech. Based Des. Struct. Mach. (2022). https://doi.org/10.1080/15397734.2022.2117194.
12. Ferreira A. J. M., Roque C. M. C. and Jorge R. M. N. - Analysis of composite plates by trigonometric shear deformation theory and multiquadrics, Comput. Struct. **83** (2005) 2225-2237.
13. Nguyen D. K., Vu A. N. T., Pham V. N. and Truong T. T. - Vibration of a three-phase bidirectional functionally graded sandwich beam carrying a moving mass using an enriched beam element, Eng. Comput. (2021). https://doi.org/10.1007/s00366-021-01496-3.
14. Šolín P. - Partial differential equations and the finite element method, Wiley, Hoboken, 2006.
15. Daghigh H. and Daghigh V. - Free Vibration of Size and Temperature-Dependent Carbon Nanotube (CNT)-Reinforced Composite Nanoplates With CNT Agglomeration, Polym. Compos. **40** (S2) (2019) E1479-E1494.
16. Yas M. H. and Heshmati M. - Dynamic analysis of functionally graded nanocomposite beams reinforced by randomly oriented carbon nanotube under the action of moving load, Appl. Math. Model **36** (2012) 1371-1394.